Toronto Metropolitan University

AER 710: Aerospace Propulsion

Final Report

Supersonic Engine Design

Student Name: Aman Gilani
Student No.: 500879895
Program: Aerospace Engineering.

Abstract

The purpose of this project was to create a supersonic inlet for a turbojet with an afterburner in order to improve the pressure recovery ratio across the diffuser. This was accomplished by placing a series of three equal-strength oblique shocks followed by a normal shock at the tip of the engine nacelle. The pressure recovery ratio calculated across the diffuser was 0.9339. The second part of this design project involved performing a non-ideal parametric cycle analysis on the designed fictional turbojet engine with an afterburner. The engine also has a converging-diverging nozzle, which allows it to maintain supersonic exit speeds. The engine was divided into several sections. Due to friction, heat transfer, and other compressor and turbine losses, sections 2–6 were assumed to be non-isentropic and non-adiabatic. As a result, the stagnation conditions at each stage were calculated using the non-ideal parametric cycle analysis.

This aircraft's design process is divided into two stages. The first section focuses on the design and optimization of the engine's supersonic inlet. The Oswatitsch Principle is used for optimization, and then a comprehensive parametric cycle analysis is performed to study its performance parameters. The second part of this project compares an off-the-shelf engine to the designed fictional engine through a trade study. This analysis compares the performance characteristics of the two engine options. The performance characteristics of the fictional engine are compared to those of a commercially available engine. The Olympus 593 engine is used as a reference aircraft because it is also a turbojet engine with a supersonic afterburner. The fictional engine generates about 185 kN of net thrust, while the Olympus 593 generates about 170 kN of net thrust. The fictional engine has a thermal efficiency of 48% and a propulsive efficiency of 70%. The fictional engine has a specific thrust of 675 N/(kg/s). The inlet and exit areas of the fictional engine and Olympus 593 are similar. The fictional engine has a 34% overall efficiency, while the Olympus 593 has a 26% overall efficiency.

Table of Contents

List of Figures

List of Tables

1. Project Description

The objective of this project is to develop and analyze a supersonic inlet for a supersonic commercial aircraft that would fly from New York to London in under three hours. The design process for this aircraft is broken into two parts. The first part focuses on the design and optimization of the supersonic inlet for the engine. The optimization is done using the Oswatitsch Principle following which a comprehensive parametric cycle analysis is to be conducted to study its performance parameters. The second part of this project focuses on performing a trade study to compare an off-the-self engine with the designed fictional engine. This analysis is completed to compare the performance characteristics of the two engine choices.

The second part of the project requires the implementation of a non-ideal parametric cycle analysis for the fictional turbojet engine. The analysis is done to calculate the stagnation conditions at each section of a turbojet engine with an afterburner along with the performance parameters for the fictional engine. These parameters are compared with the performance characteristics of the Olympus 593 engine used on the Concorde airplane. The objective of this design project is to apply the knowledge of gas dynamics and propulsion of turbojet engines to design a fictional engine and compare its performance characteristics to an off-the-shelf engine.

2. Approach

The first task pertains to the preliminary design of the supersonic inlet for the fictional engine. The supersonic inlet of the engine decelerates the incoming flow to subsonic speeds through a suitable shock system. For this project, the aim is to design an optimal shock system consisting of three oblique shocks followed by a normal shock. The primary objective for doing this is to optimize the inlet for the ideal pressure recovery ratio (π_d). The flight Mach number (M_1) is given as 2.4 and the normal shock up-stream Mach number (M_4) is given as 1.3. The following section will focus on the equations and methodology used to complete the given tasks.

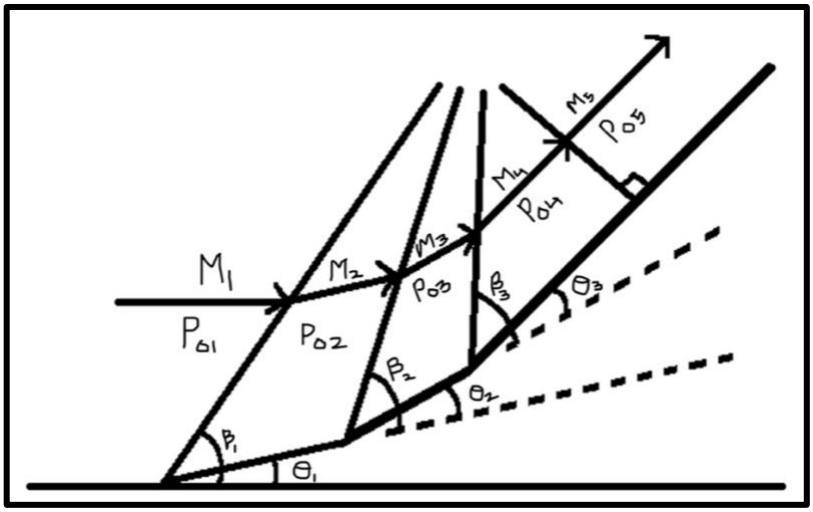

Figure 1: Multi Shock Compression for Oswatitsch Optimization.

2.1 Supersonic Inlet Design

The preliminary design of the supersonic inlet is completed keeping in mind the objective to optimize the inlet pressure recovery ratio. For the given system of shocks, as represented in figure 1, Oswatitsch's Principle is used to optimize the flow in the supersonic inlet. According to Oswatitsch's principle, the pressure recovery in a system of $(n-1)$ oblique shocks followed by the nth normal shock (see Fig. 1) is maximum when the shocks are of equal strength, i.e., that is upstream Mach numbers normal to the oblique shocks are equal. This concept is represented in *equation 1* below.

$$M_1 \sin(\beta_1) = M_2 \sin(\beta_2) = M_3 \sin(\beta_3) \qquad \textit{Equation 1}$$

Following defining the problem statement and the objectives, a set of equations are developed for the system of shocks. The equation below relates the normal component of M_1 upstream of the oblique shock with the shock wave angle. Integrating Oswatitsch's Principle it was observed that the normal component of the upstream Mach number for all oblique shocks are equal. This is also represented in *equation 1* ($M_{1n} = M_{2n} = M_{3n}$).

$$M_{1n} = M_1 \sin(\beta_1) \qquad \textit{Equation 2}$$

The equation below represents the relation between normal component of M_1 downstream of the oblique shock with the normal component of M_1 upstream of the oblique shock. This relationship is variable with the change in specific heat ratio (γ). For this project, the ratio was given as 1.4.

$$M_{1n2} = \sqrt{\frac{M_{1n}^2 + \frac{2}{\gamma-1}}{\frac{2\gamma}{\gamma-1}M_{1n}^2 - 1}}$$ *Equation 3*

The equation below relates the deflection angle to the wave angle (β_1) and Mach number (M_1). The deflection angle is the angle by which the incoming flow is deflected. The value for this angle corresponds to a different combination of wave angle and Mach number.

$$\theta_1 = tan^{-1}\left[\frac{2\,cot(\beta_1)({M_1}^2(sin\,\beta_1)^2 - 1)}{(\gamma+1)*{M_1}^2 - 2({M_1}^2(sin\,\beta_1)^2 - 1)}\right]$$ *Equation 4*

The Following equation is used to compute the downstream Mach number (M_2). This Mach number depends on the normal component (M_{1n2}) calculated in *equation 3*, the deflection angle calculated in *equation 4,* and the wave angle calculated using Oswatitsch's principle.

$$M_2 = \frac{M_{1n2}}{sin(\beta_1 - \theta_1)}$$ *Equation 5*

The following equations *(6 and 7)* are used to calculate the stagnation pressure ratios and total pressure ratios across individual shocks present in the given system respectively. These pressure ratios depend on the normal component of the upstream Mach number. Integrating Oswatitsch's Principle it was discovered that the pressure ratios across oblique shocks one, two and three are equal ($\frac{P_2}{P_1} = \frac{P_3}{P_2} = \frac{P_4}{P_3}$) and ($\frac{P_{02}}{P_{01}} = \frac{P_{03}}{P_{02}} = \frac{P_{04}}{P_{03}}$). This is because the oblique shocks are of the same strength.

$$\frac{P_2}{P_1} = \frac{2\gamma M_{1n}^2}{\gamma+1} - \frac{\gamma-1}{\gamma+1}$$ *Equation 6*

$$\frac{P_{02}}{P_{01}} = \left[\frac{\frac{\gamma+1}{2}M_{1n}^2}{1+\frac{\gamma-1}{2}M_{1n}^2}\right]^{\frac{\gamma}{\gamma-1}}\left[\frac{1}{\frac{2\gamma M_{1n}^2}{\gamma+1} - \frac{\gamma-1}{\gamma+1}}\right]^{\frac{1}{\gamma-1}}$$ *Equation 7*

The following relationship is used to calculate the intake pressure recovery ratio (π_d). This ratio is optimized using Oswatitsch's Principle for ($n - 1$) oblique shocks followed by the nth normal shock.

$$\pi_d = \frac{P_{05}}{P_{01}} = \frac{P_{02}}{P_{01}} * \frac{P_{03}}{P_{02}} * \frac{P_{04}}{P_{03}} * \frac{P_{05}}{P_{04}}$$ *Equation 8*

The above-derived equations are used for subsequent oblique shocks. These equations are then solved using the '*vpasolve*' function in MATLAB. The code for this is included in Appendix

A. The results of this optimization process are included in the final design section with a rendition of the resultant inlet geometry.

2.2 Parametric Analysis

Following designing the supersonic inlet for the fictional turbojet, the parametric cycle analysis is completed for the engine to obtain the thrust, performance, and efficiency parameters. The following figure illustrates the turbojet engine with an afterburner. The afterburner is included in the engine to provide additional thrust.

A non-ideal parametric cycle analysis of a supersonic turbojet with an afterburner entails a conceptual study of engine performance under non-ideal conditions. The study considers the various sources of losses and inefficiencies in engine components and the combustion process. The engine's intake process involves compressing air to a high-pressure ratio. Factors such as pressure recovery, shock losses, boundary layer effects, and turbulence all have an impact on diffuser efficiency. Similarly, compressor efficiency, pressure losses, and leakage all have an impact on the compression process. The combustion process is one of the most important stages in the engine cycle because it determines how much heat is released and the temperature of the exhaust gases. The combustion process's efficiency is influenced by factors such as combustion chamber design, fuel injection system, mixing efficiency, and flame stabilization. The expansion process involves the expansion of exhaust gases through the turbine to generate work and thrust. Factors such as turbine blade design, blade cooling, and nozzle efficiency all have an impact on turbine efficiency. A non-ideal analysis includes the afterburner stage, which involves injecting fuel into the exhaust gases to generate additional thrust. Factors such as mixing efficiency, flame stabilization, and pressure losses all have an impact on afterburner efficiency.

The engine's performance is measured using various parameters such as thermal efficiency, propulsive efficiency, and specific thrust. The thermal efficiency is the ratio of the engine's net work to the heat input, whereas propulsive efficiency is the ratio of the engine's propulsive work to the total work input. The specific thrust is the ratio of thrust produced to the air flow rate through the engine.

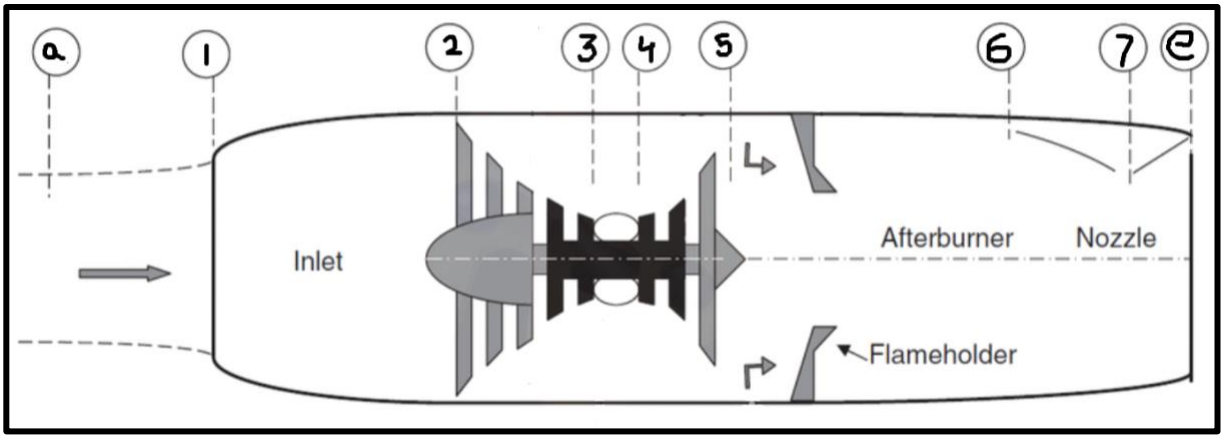

Figure 2: Cross-Section of Engine Stations.

The parametric cycle analysis for the engine was divided into 7 sections. The following equations *(9 and 10)* are used to calculate the stagnation pressure and temperature at the inlet of the diffuser. The section from 'a' to '1' is assumed to be isentropic and thus the stagnation pressure and temperature at '1' are assumed to be equal to the ambient stagnation conditions.

$$P_{o1} = P_{oa} = P_{amb} * \left(1 + \frac{\gamma_d - 1}{2} * M_a^2\right)^{\frac{\gamma_d}{\gamma_d - 1}} \quad \textit{Equation 9}$$

$$T_{o1} = T_{oa} = T_{amb} * \left(1 + \frac{\gamma_d - 1}{2} * M_a^2\right) \quad \textit{Equation 10}$$

The stagnation conditions at '2', which is the inlet of the compressor, are calculated using the following equations *(11 and 12)*. The diffuser pressure ratio (π_d) was calculated from the supersonic diffuser section above (*Equation 8*). Sections 2 to 6 are considered to be non-isentropic and non-adiabatic. This entails that there are losses in the entropy ad total pressure due to several reasons mentioned above.

$$P_{o2} = P_{o1} * \pi_d \quad \textit{Equation 11}$$

$$T_{o2} = T_{o1} * (\pi_d)^{\frac{\gamma_d - 1}{\gamma_d}} \quad \textit{Equation 12}$$

The stagnation conditions at '3', which is the inlet for the burner, are calculated using the following equations *(13 and 14)*. The compressor pressure ratio (π_c) was deducted from historic data for similar turbojet engines.

$$P_{o3} = P_{o2} * \pi_c \quad \textit{Equation 13}$$

$$T_{o3} = T_{o2} * \left(1 + \frac{(\pi_c)^{\frac{\gamma_c - 1}{\gamma_c}} - 1}{\eta_c}\right)$$ *Equation 14*

The stagnation pressure at '4', which is the inlet for the turbine, is calculated using the following equations (*15*). The compressor pressure ratio (π_b) was deducted from historic data for similar turbojet engines. The stagnation temperature at '4' was deducted from the temperature limit for turbine blades. Although the stagnation temperature $'T_{o4}'$ could be higher than the turbine temperature limit while using active cooling concepts. However, this wasn't considered for the scope of this project to make the calculations simpler.

$$P_{o4} = P_{o3} * \pi_b$$ *Equation 15*

The fuel-to-air ratio of the burner is calculated using the following equations (*16 and 17*). The specific heat ratio for this section is different from that of the compressor, turbine, and nozzle. This is because the temperatures in the burner are significantly higher than in the other mentioned sections of the engine. The fuel-to-air ratio in the burner is essential because it dictates the combustion efficiency, fuel consumption, and harmful emissions. The higher the fuel-to-air ratio the higher the emissions, and the higher the power output.

$$C_{p,Component} = \frac{\gamma_{component}}{\gamma_{component} - 1} * R_{air}$$ *Equation 16*

$$f_b = \frac{\frac{T_{o4}}{T_{o3}} - \frac{C_{p,c}}{C_{p,be}}}{\frac{\eta_b * q_R}{C_{p,be} * T_{o3}} - \frac{T_{o4}}{T_{o3}}}$$ *Equation 17*

The stagnation conditions at '5', which is the inlet for the afterburner, are calculated using the following equations (*18 and 19*). Since the flow is considered to be non-adiabatic across the turbine, the stagnation conditions at the afterburner inlet account for the mechanical (frictional) losses for the turbomachinery bearing.

$$T_{o5} = T_{o4} - \frac{T_{o3} - T_{o2}}{\eta_m}$$ *Equation 18*

$$P_{o5} = P_{o5} * \left(1 - \frac{1}{\eta_t}\left(1 - \frac{T_{o5}}{T_{o4}}\right)\right)^{\frac{\gamma_t}{\gamma_t - 1}}$$ *Equation 19*

The fuel-to-air ratio for the afterburner is calculated using *Equation 20.* The fuel-to-air ratio in the afterburner is essential because it influences the additional thrust output of the engine, combustion

efficiency, fuel consumption, and harmful emissions. The higher the fuel-to-air ratio the higher the emissions, and the higher the power output.

$$f_{a/b} = \frac{\frac{T_{06}}{T_{05}} - \frac{C_{p,t}}{C_{p,a/be}}}{\frac{\eta_{a/b} * q_R}{C_{p,a/be} * T_{05}} - \frac{T_{06}}{T_{05}}} \qquad \textit{Equation 20}$$

The static conditions at exit are calculated using the following equations (21, 22, 23, and 24). The conditions in the converging–diverging nozzle are considered to be isentropic and adiabatic. Furthermore, the nozzle areas are designed for the throat to be choked. As seen in the pressure ratio map (*figure 3*) below, the flow expands as it reaches Mach 1 at the throat and the velocity increases as the flow exits the nozzle and the pressure decreases.

$$P_e = \frac{P_{06}}{\left(1 + \frac{\gamma_n - 1}{2} * M_e^2\right)^{\frac{\gamma_n}{\gamma_n - 1}}} \qquad \textit{Equation 21}$$

$$A_{Throat} = \frac{A_{Exit}}{\frac{1}{M_e}\left(\frac{2}{\gamma_n + 1} * \left(1 + \frac{\gamma_n - 1}{2} * M_e^2\right)\right)^{\frac{\gamma_n - 1}{2(\gamma_n + 1)}}} \qquad \textit{Equation 22}$$

$$T_e = \frac{T_{06}}{1 + \frac{\gamma_n - 1}{2} * M_e^2} \qquad \textit{Equation 23}$$

$$V_e = M_e * \sqrt{\gamma_n * R * T_e} \qquad \textit{Equation 24}$$

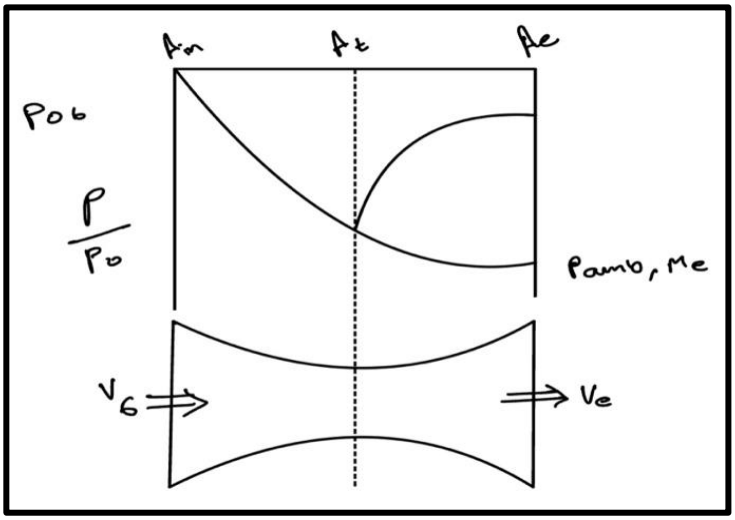

Figure 3: Converging - Diverging Nozzle Pressure Map.

The designed fictional engine and the off-the-shelf engine is compared using the following performance characteristics. The two engines are compared using the specific thrust, thrust-specific fuel consumption, mass flow rates, thrust, and efficiencies. These parameters are calculated using the following equations (*26 - 34*).

$$\frac{A_e}{\dot{m}} = \left(\frac{\gamma_n+1}{2}\right)^{\frac{1}{\gamma_n-1}} * \left(\frac{\gamma_n+1}{2\gamma_n RT_{o6}}\right)^{0.5} * \left(\frac{RT_{o6}}{P_{o6}}\right) \quad \textit{Equation 25}$$

$$Specific\ Thrust = \frac{F}{\dot{m}_a} = \left(1 + f_b + f_{a/b}\right) * V_e - V_\infty + \frac{A_e}{\dot{m}}(P_e - P_\infty)\left(1 + f_b + f_{a/b}\right) \quad \textit{Equation 26}$$

$$TSFC = \frac{f_b + f_{a/b}}{\frac{F}{\dot{m}_a}} \quad \textit{Equation 27}$$

$$\dot{m}_a = \rho_{amb} * A_{in} * V_{in} \quad \textit{Equation 28}$$

$$\dot{m}_f = \dot{m}_a * (f_b + f_{a/b}) \quad \textit{Equation 29}$$

$$\dot{m}_e = \dot{m}_a + \dot{m}_f \quad \textit{Equation 30}$$

$$Thrust = \frac{F}{\dot{m}_a} * \dot{m}_a \quad \textit{Equation 31}$$

The thermal efficiency for a turbojet with an afterburner is hypothesized to be from 30% – 50%. The propulsive efficiency for a turbojet with an afterburner is hypothesized to be from 70% – 80%.

$$\eta_{th} = \frac{\left(1+f_b+f_{a/b}\right)*V_e^2 - V_\infty^2}{2*\left(f_b + f_{\frac{a}{b}}\right)*q_R} \quad \textit{Equation 32}$$

$$\eta_p = \frac{2*\frac{F}{\dot{m}_a}*V_\infty}{\left(1+f_b+f_{a/b}\right)*V_e^2 - V_\infty^2} \quad \textit{Equation 33}$$

$$\eta_o = \eta_p * \eta_{th} \quad \textit{Equation 34}$$

3. Final Design

For the preliminary design of the supersonic inlet, *equations 1 through 8* are used to optimize the inlet using Oswatitsch's Principle. With the given values for M_1, M_4 and γ as 2.4, 1.3 and 1.4 respectively, the equations for normal components M_{1n} , M_{2n} and M_{3n} were derived similar to *equation 2*. Similarly, equations for normal components M_{1n2} , M_{2n2} and M_{3n2} were derived similar to *equation 3*. Deflection angles for each oblique shock θ_1, θ_2 and θ_3 were derived using *equation 4*. Following this, the equations for upstream Mach numbers for each oblique shock M_1 ,M_2 and M_3 were derived using *equation 5*. Afterward, the upstream normal components of Mach numbers are equated using Oswatitsch's Principle. The symbolic equations are then solved simultaneously using the '*vpasolve*' function in MATLAB. The results of this optimization are tabulated in *Table 1*.

The non–ideal parametric cycle analysis for the designed turbojet with an afterburner is completed using equations presented in the above subsection. The Net Thrust produced by the engine is 287 kN with an exit Mach number of 2.62. The engine has a thermal efficiency of 48.4 %, propulsive efficiency of 70.7 %, and an overall efficiency of 34.2%. The design parameters for the fictional engine are presented in *Table 2* and *Table 3*. The non–ideal parametric cycle analysis was completed using MATLAB live script and the code is presented in Appendix A.

3.1 Supersonic Inlet Design

The following *Table (1)* tabulates the results of the optimization of the supersonic inlet completed in MATLAB. The optimized pressure recovery ratio was calculated to be 0.9339. The inlet rendition for the designed engine is illustrated in *Figure 4*. This rendition features a series of oblique shocks followed by a normal shock. The presence of shocks slows down the incoming supersonic flow whilst optimizing the pressure recovery across the diffuser. The shock angles and their respective deflection angles and pressure ratios are presented in *Table 1*.

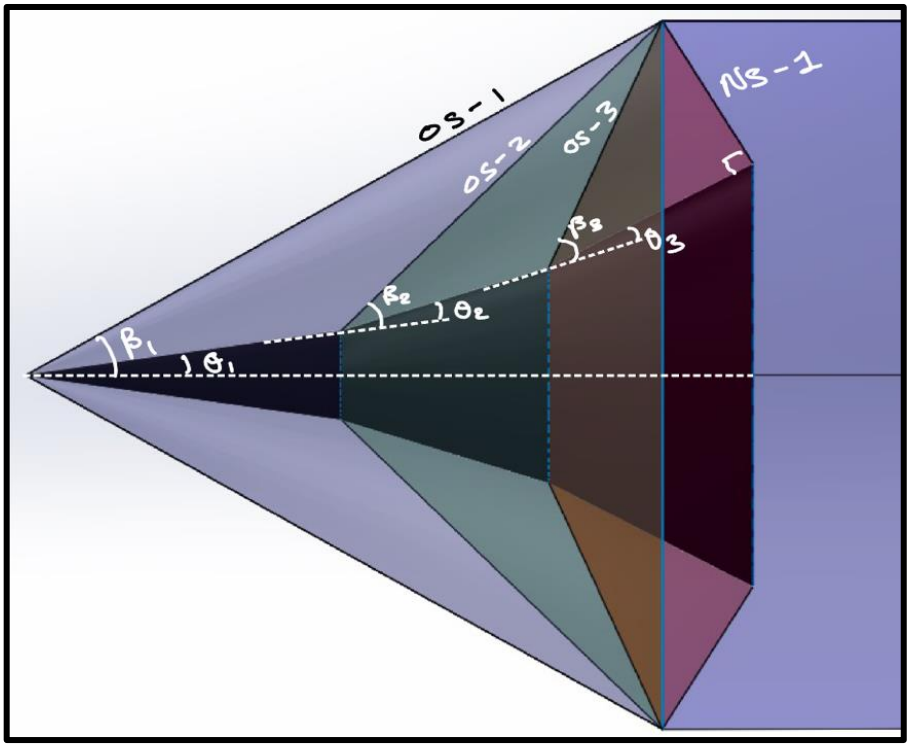

Figure 4: Inlet – Diffuser Rendition with Shocks.

The *Figure 4* illustrates the inlet rendition featuring a series of oblique shocks followed by a normal shock. The calculated $M_1, M_2, M_3,$ and M_4 are 2.4, 2.0454, 1.6847, and 1.3 respectively. The calculated wave angles $\beta_1, \beta_2,$ and β_3 are 31.9353, 38.3646, and 48.8981 respectively. The Calculated deflection angles $\theta_1, \theta_2,$ and θ_3 are 8.853, 9.9409, and 10.8113 respectively. The calculated pressure recovery ratio (π_d) is 0.9339.

Table 1: Calculated Values for Supersonic Inlet Design.

Mach Numbers	Calculated Values
M_1	2.4000
M_2	2.0454
M_3	1.6847
M_4	1.3000
Wave Angles	**Calculated Values (deg)**
β_1	31.9353
β_2	38.3646
β_3	48.8981
Deflection Angles	**Calculated Values (deg)**
θ_1	8.8530
θ_2	9.9409
θ_3	10.8113

Static Pressure Ratios	Calculated Values
$\frac{P_2}{P_1} = \frac{P_3}{P_2} = \frac{P_4}{P_3}$	1.7136
$\frac{P_5}{P_4}$	1.8050
Static Temperature Ratios	**Calculated Values**
$\frac{T_2}{T_1} = \frac{T_3}{T_2} = \frac{T_4}{T_3}$	1.1716
$\frac{T_5}{T_4}$	1.1909
Total Pressure Ratios	**Calculated Values**
$\frac{P_{o2}}{P_{o1}} = \frac{P_{o3}}{P_{o2}} = \frac{P_{o4}}{P_{o3}}$	0.9843
$\frac{P_{o5}}{P_{o4}}$	0.9794
Inlet Pressure Recovery ratio	**Calculated Values**
$\boldsymbol{\pi_d = \frac{P_{o5}}{P_{o1}}}$	**0.9339**

3.2 Parametric Analysis

This section presents the premise and results for the non – ideal parametric cycle analysis conducted for designed turbojet engine. The engine is designed to with a cruising/operating altitude of 51,000 ft. This is in accordance with the FAA's regulation for the maximum operating altitude for turbojets. Since the inlet for the designed engine is supersonic (Mach 2.4) and the flight speed for the turbojet is supersonic, the cruising altitude of 51,000 ft. would give a beneficial boost in engine performance in maintaining supersonic speed and reduce profile drag on the aircraft. A rendition for the designed engine is presented in *Figure 5*. The turbojet engine features an afterburner for an increase in thrust at the chosen altitude. The engine is divided into six sections, which are as follows: Inlet & Diffuser, Single Spool Compressor, Burner, Single Spool Turbine, Afterburner, and Converging – Diverging Nozzle. The turbojet cycle was completed considering the non–ideal assumption as the section themselves operate at a certain efficiency. As mentioned above, the process in sections 1 to 6 is considered to be non – isentropic and non–adiabatic. Therefore, the stagnation temperatures and pressures at each section inlet are not constant. Furthermore, that is why the specific heat ratios for each section are not constant.

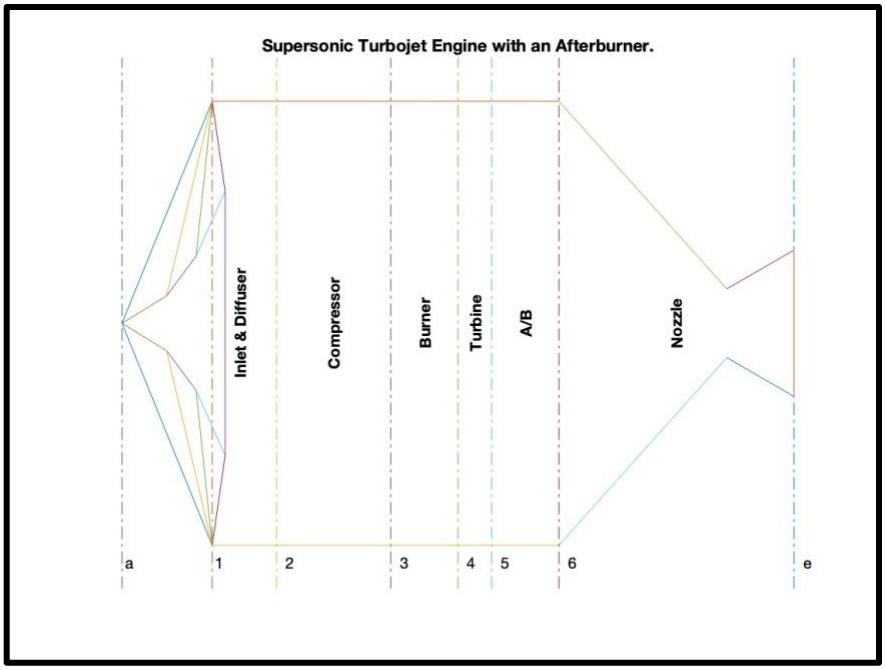

Figure 5: Engine Cross-Sectional Rendition.

The diffuser pressure ratio is 0.9339 and calculated from the supersonic inlet design in the previous section. The compressor pressure ratio is 10 and is deduced from engines operating in a similar category. From a similar data set, the compressor is presumed to be operating at 90% efficiency. The burner pressure ratio is deduced to be 0.95 and its efficiency at 99%. This pressure ratio was determined keeping in consideration that the process is non-isentropic, and the pressure drop accounts for losses such as heat transfer to the surrounding sections, frictional losses in the duct, and incomplete combustion of the fuel. The A-1 Kerosene Jet fuel with a heating value of 43,390 kJ/kg is used for the combustor calculations. The maximum temperature in the burner is in ordinance with the maximum temperature for the turbine blades. This is a design choice when implementing the parametric analysis for the turbojet engine because the engine is not designed with any active cooling concepts. The maximum temperature at the burner exit is 1300 K and is deduced from the current materials used as turbine blades.

The turbine efficiency is deduced to be 95 % and the efficiency for the turbomachinery is deduced to be 99 %. An afterburner was added to the engine to provide additional thrust during various stages of the flight envelope. The thrust, performance, and efficiency values for the engine with the use of the afterburner and without are presented in *Table 3*. With the use of the afterburner, the engine produces approximately 47.5% additional thrust. The afterburner pressure ratio is

deduced to be at .95 and its efficiency is at 95 %. The maximum temperature for the afterburner is also a design parameter. For the designed engine, this temperature was deduced to be 1500 K. As seen in *Figure 5*, the designed nozzle has a converging–diverging geometry. The Pressure map in *Figure 4,* describes the flow through the nozzle. The throat is choked, and the design exit Mach number is 2.62. The nozzle is designed such that the exit static pressure is equal to the ambient static pressure at the chosen cruise altitude.

Table 2: Turbojet Pressure and Temperature Ratio Across Stations.

Parameter		Calculated Value
Ambient	P_{oa}	161.6 kPa
	T_{oa}	466.2 K
	P_e	11.0 kPa
	T_e	216.6 K
Compressor	P_{o2}	150.9 kPa
	T_{o2}	457.2 K
Combustion Chamber	P_{o3}	1509.1 kPa
	T_{o3}	895.3 K
Turbine	P_{o4}	1433.7 kPa
	T_{o4}	1300 K
Afterburner	P_{o5}	239.8 kPa
	T_{o5}	857.5 K
Nozzle	P_{o6}	227.8 kPa
	T_{o6}	1500 K
Exit	P_{oe}	227.8 kPa
	T_{oe}	1500 K
	P_e	10.05 kPa
	T_e	670.7 K

The *Table 2* tabulates the stagnation conditions at each engine section. The static ambient conditions are obtained for the chosen cruising altitude and the stagnation ambient conditions are calculated from *Equation 9* and *Equation 10*. The compressor inlet stagnation pressure and temperature are 50.9 kPa and 457 K respectively. Using the compressor pressure ratio of 10, the combustion chamber inlet stagnation pressure and temperature are 1509.1 kPa and 895.3 K respectively. The turbine inlet stagnation pressure and temperature are 1433.7 kPa and 1400 K respectively. The afterburner inlet stagnation pressure and temperature are 239 kPa and 857 K respectively. The nozzle inlet stagnation pressure and temperature are 227 kPa and 1500 K

respectively. The Nozzle is designed as isentropic and fully expanded with an exit Mach number of 2.62. The Exit static pressure and temperature are calculated to be 10.05 kPa and 670 K respectively.

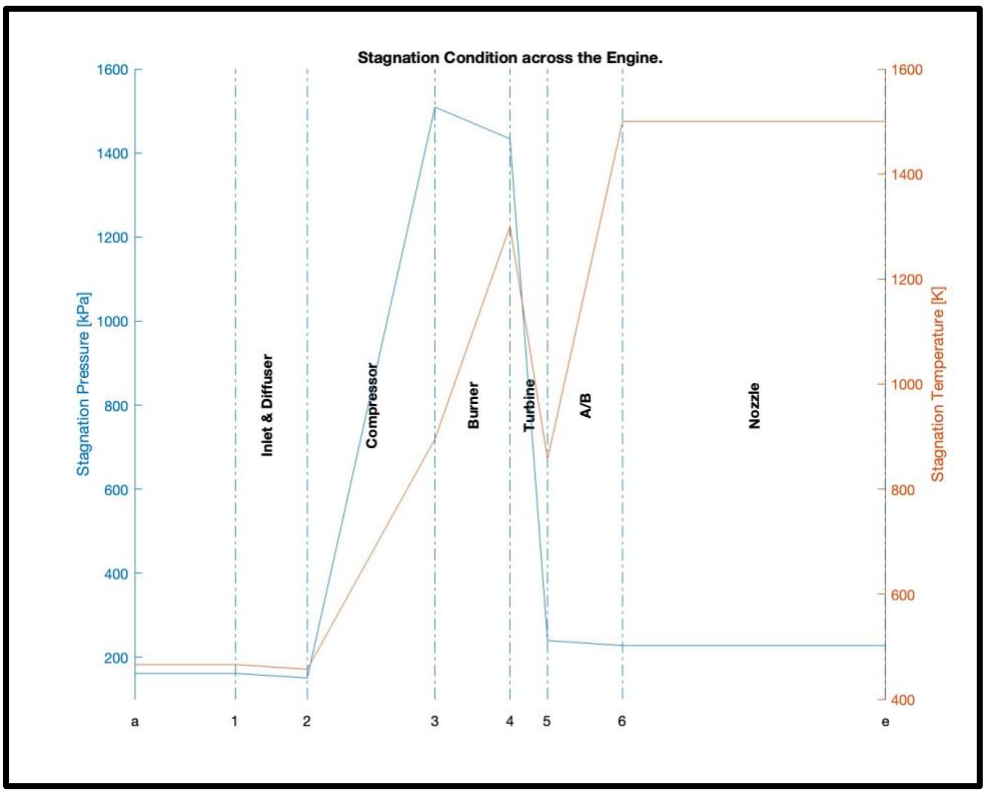

Figure 6: Stagnation Pressure and Temperature Changes Across the Engine.

Figure 6 above illustrates the variation of stagnation pressure and stagnation temperature across the engine. As the flow starts from the inlet, it goes through a series of oblique shocks followed by a normal shock. Through this section (*a – 1*) the stagnation pressure drops since the flow are non-isentropic whereas the stagnation temperature remains constant since the flow is adiabatic. However, the diffuser (*1 – 2*) is considered to be non-ideal and therefore the stagnation pressure and temperature drop are recorded. Following the flow through the compressor section (*2 – 3*), the stagnation pressure increases as well as the temperature. This is because the flow is slowed and compressed for the burner to operate optimally. The flow through the burner section (*3 – 4*) is non-isentropic and non-adiabatic. The heat addition in the burner section is considered to be non – ideal and therefore the losses account for heat transfer to other sections and friction. The turbine section (*4 – 5*) accounts for the maximum stagnation pressure drop in the engine. This is because the flow accelerates through this section and the energy extracted from the flow is used to power

the compressor. When operated without the afterburner, the engine produces 47.5 % less thrust as compared when operated with an afterburner. The increase in thrust is accounted for by the increase in stagnation pressure across the afterburner section (*5 – 6*). The flow across the nozzle section (*6 – e*) is isentropic and adiabatic. Furthermore, the converging–diverging nozzle is designed to fully expand at its operating altitude.

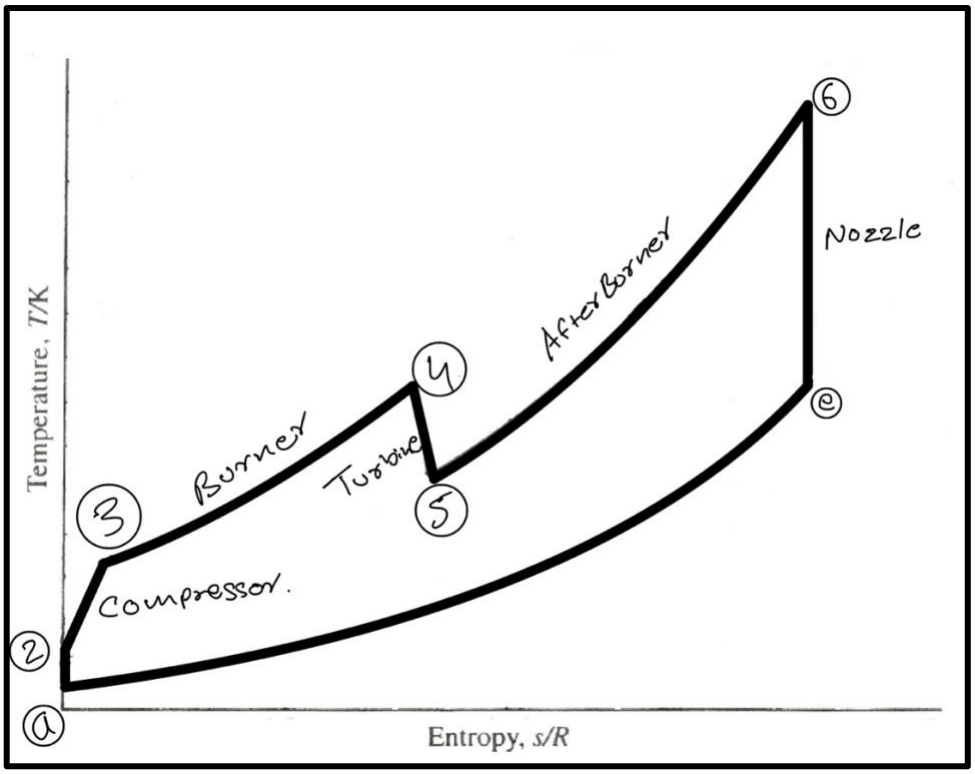

Figure 7: Temperature Vs. Entropy Diagram for Non-Ideal Turbojet Cycle.

Figure 7 illustrates the non-ideal turbojet cycle for the designed engine. Sections *a to 2* is isentropic and adiabatic which are shown using a straight line. Since the sections are non-ideal from *2 to 6*, they are also non-adiabatic and non-isentropic. As evidenced in *Figure 6* and *Figure 7,* the stagnation temperature and stagnation pressure are not constant and represented with curved lines. Section *6 to e* for the nozzle is considered to be isentropic and adiabatic and therefore represented with a straight line. The loss in entropy is accounted for by various types of compressor and turbine losses, combustion losses, pressure losses, and heat losses.

Table 3: Non–Ideal Turbojet Parametric Cycle Analysis.

Parameter		Calculated Value
Ambient	M_a	2.4
	Altitude	51,000 Ft.
Exit	M_e	2.621
	V_e	1341 m/s
Thrust **With A/B**	Net Thrust	187 kN
	Gross Thrust	383.3 kN
Thrust **Without A/B**	Net Thrust	88.8 kN
	Gross Thrust	284.4 kN
Efficiency **With A/B**	η_{th}	48.4 %
	η_{Pr}	70.6 %
	η_o	34.2 %
Efficiency **Without A/B**	η_{th}	47.3 %
	η_{Pr}	84.1 %
	η_o	39.8 %
Mass Flow Rates	$\dot{m}_a$	276.9 kg/s
	$\dot{m}_f$	8.9 kg/s
	$\dot{m}_e$	285.8 kg/s
Area	A_{in}	2.2 m^2
	A_e	0.75 m^2
Performance **With A/B**	Specific Thrust	676 N/(kg/s)
	TSFC	0.00004766 (kg/s)/N
Performance **Without A/B**	Specific Thrust	321 N/(kg/s)
	TSFC	0.00004099 (kg/s)/N

The *Table 3* above tabulates the results for the non – ideal parametric cycle analysis conducted for the designed turbojet with and without an afterburner. The design exit Mach number is 2.62. The net and gross thrust for engine when operating with an afterburner is 187 kN and 383 kN respectively. When the engine is operated without an afterburner, the net thrust decreases by approximately 47.5 %. The thermal efficiency and propulsive efficiency of the engine when operating with an afterburner are 48.4 % and 70.6 % respectively. When the engine is operating without an afterburner, the thermal efficiency decreases whereas the propulsive efficiency increased significantly. The mass flow rate of the exhaust gases increases when an afterburner is used, but the mass flow rate of the air entering the engine remains constant. As a result, the engine's

output is directed towards heating the exhaust gases rather than providing thrust, resulting in lower propulsive efficiency with the afterburner.

The Overall efficiency of the engine when operating with an afterburner is 34.3 %. This overall efficiency increases when the afterburner is not used. The specific thrust and TSFC for the engine when operating with an afterburner are 676 N//(kg/s) and 0.00004766 (kg/s)/N respectively. The specific thrust and TSFC decrease when the engine is operated without an afterburner. This is because the thrust decreases when an afterburner is not used whereas the mass flow rate remains constant.

4. Design Comparison

In this section, the designed engine is compared with an off-the-shelf engine. The off-the-shelf engine considered for this project is the Olympus 593 Engine used on the Concorde. The Olympus 593 is a turbojet engine cable of maintaining supersonic speeds at cruise. Furthermore, the operating altitude for this engine is in accordance with the designed engine. The Olympus engine has an inlet and exit area of 2.2 m^2 and 0.74 m^2 respectively. To compare the two engines reasonably, the fictional engine is also designed to have the same similar areas as tabulated in *Table 4*. The operating inlet Mach number for the Olympus engine is 3.4 and the operating inlet Mach number of the fictional engine is 2.4 as constrained by the design statement. The calculated exit velocity of the Olympus engine is approximately 1700 m/s and the exit velocity for the fictional engine is approximately 1300 m/s. The fictional engine has a significantly smaller specific thrust as compared to the Olympus 593 engine. The specific thrust for the fictional engine is 670 N/(kg/s) and the Olympus 593 engine has a specific thrust of 19,000 N/(kg/s). The thrust-specific fuel consumption (TSFC) for the fictional engine and the Olympus engine are 0.05 (kg/s)/kN and 0.0008 (kg/s)/kN respectively. This entails that the fictional engine has a higher mass flow rate as compared to the Olympus engine.

The thermal efficiency and the propulsive efficiency of the fictional engine are 48% and 60% respectively. The thermal efficiency and propulsive efficiency of the Olympus engine are 40% and 65% respectively. As recorded in *Table 4*, the designed fictional engine has higher efficiencies as compared to the Olympus 593 engine. The net thrust produced by the fictional engine is 185 kN and the thrust produced by the Olympus 593 engine is 170 kN.

Table 4: Engine Comparison between the 'Designed Fictional' and 'Olympus 593.

Parameter		Fictional Engine	Olympus 593 Engine
Areas	Inlet Area	2.2 m^2	2.2 m^2
	Exit Area	0.75 m^2	0.74m^2
Performance	M_a	2.4	3.4
	V_e	1341 m/s	1700 m/s
	Specific Thrust	676 N/(kg/s)	19,000 N/(kg/s)
	TSFC	0.04766 (kg/s)/kN	0.0008 (kg/hr)/kN
Efficiency	η_{th}	48.4 %	40 %
	η_{Pr}	70.6 %	65 %
	η_o	34.2 %	26 %
Thrust	Net Thrust	187.2 kN	170 kN

5. Future Recommendations

The designed fictional engine shows promise after conducting the non–ideal parametric cycle analysis. As seen in the above section, the net thrust calculated for the fictional engine is higher than Olympus 593 engine. However, the performance of an engine does not solely depend on this analysis. It is recommended that an extensive future analysis, specifically on the aerodynamics and thermodynamics of the engine is carefully conducted and evaluated. The fictional engine was recorded to have a lower thrust generation to mass flow rate ratio. This could be optimized by increasing the maximum temperatures in the burner and the afterburner. This would provide a significant increase in thrust whilst maintaining a relatively constant mass flow rate. Similarly, the thrust-specific fuel consumption for the fictional engine can be optimized by optimizing the fuel-burning temperatures and designing the nozzle to optimize the exit velocity at various stages of the flight envelope. The inlet and nozzle can also be redesigned with variable areas to make the engine more adaptable and efficient at various altitudes. Finally, the fictional engine is a good starting point to build an optimized version that keeps into consideration various other aspects of supersonic flight and aircraft performance.

6. Conclusion

The objective of this project was to design a supersonic inlet for a turbojet with an afterburner with the intention of optimizing the pressure recovery ratio across the diffuser. This was achieved by placing a series of 3 oblique shocks of equal strength followed by a normal shock at the tip of the engine nacelle as shown in *Figure 4*. The pressure recovery ratio across the diffuser was calculated to be 0.9339. The second part of this design project was to conduct a non–ideal parametric cycle analysis of the designed fictional turbojet engine with an afterburner. The engine also features a converging–diverging nozzle for the engine to maintain supersonic exit speeds. The engine was divided into various sections as seen in *Figure 2*. Sections 2 to 6 were assumed to be non-isentropic and non-adiabatic due to the losses in friction, heat transfer, and other compressor and turbine losses. Therefore, using the non–ideal parametric cycle analysis, the stagnation conditions at each stage were calculated and are presented in *Table 2*.

The performance characteristics of the fictional engine are then compared to an off-the-shelf engine. The Olympus 593 engine is used as a reference aircraft since it is also a turbojet engine with an afterburner capable of supersonic flight. The fictional engine produces approximately 185 kN of net thrust while the Olympus 593 produces 170 kN of net thrust. The fictional engine has a thermal and propulsive efficiency of 48% and 70% respectively. The specific thrust for the fictional engine is 675 N/(kg/s). The fictional engine and Olympus 593 both have similar inlet and exit areas. The fictional engine has an overall efficiency of 34% and the Olympus 593 has an overall efficiency of 26%.

To conclude, the designed fictional engine is a better option in terms of thrust and engine efficiency. This is because the fictional engine is optimized to generate maximum thrust by optimizing various stages of the turbojet engine. However, it is recommended that further analysis be conducted on the fictional engine to determine and analyze its thermodynamics and aerodynamic behavior.

7. References

[1] E. Karataş, "Semester Project: Supersonic Engine Design," Department of Aerospace Engineering, Toronto Metropolitan University, Toronto, 2023.

[2] D. R. Greatrix, Powered Flight the Engineering of Aerospace, London: Springer, 2012.

[3] E. Karataş, "Parametric Cycle analysis," Toronto Metropolitan University, October 2019. [Online]. Available: https://courses.torontomu.ca/d2l/le/content/716890/viewContent/4845932/View.

[4] "AIAA Foundation Student Design Competition 2022 engine special edition ..." [Online]. Available: https://www.aiaa.org/docs/default-source/uploadedfiles/education-and-careers/university-students/design-competitions/undergrad-gte-rfp---special-edition-for-2022.pdf?sfvrsn=b052fd89_0. [Accessed: 22-Mar-2023].

[5] "Airplane Flying Handbook," *Airplane Flying Handbook | Federal Aviation Administration*. [Online]. Available: https://www.faa.gov/regulations_policies/handbooks_manuals/aviation/airplane_handbook. [Accessed: 22-Mar-2023].

[6] "Technical Q&A - fuels," *International Association for Stability, Handling, and Use of Liquid Fuels, Inc.* [Online]. Available: https://iashulf.memberclicks.net/technical-q-a-fuels. [Accessed: 22-Mar-2023].

8. Appendix A

```
%{
AER 710 - Propulsion
Project 1
Aman Gilani
500879895
%}

%% Part 1 - Inlet Design.
clc
clear
close

% Given Data
M1 = 2.4;
M4 = 1.3;
gamma = 1.4;

syms M2 M3 beta1 beta2 beta3

% Upstream Normal Components of Oblique Shocks.
M1_n = M1*sind(beta1);
M2_n = M2*sind(beta2);
M3_n = M3*sind(beta3);

% Downstream Normal Components of Oblique Shocks.
M1_n2 = sqrt(((M1_n^2)+(2/(gamma-1)))/((((2*gamma)/(gamma-1))*(M1_n^2))-1));
%pretty(M1_n2)
M2_n2 = sqrt(((M2_n^2)+(2/(gamma-1)))/((((2*gamma)/(gamma-1))*(M2_n^2))-1));
M3_n2 = sqrt(((M3_n^2)+(2/(gamma-1)))/((((2*gamma)/(gamma-1))*(M3_n^2))-1));

% Surface Deflection Angles.
theta1 = atand((2*(cotd(beta1))*((M1^2)*(sind(beta1))^2-1))/((gamma +
1)*(M1^2)-2*((M1^2)*(sind(beta1))^2-1)));
%pretty(theta1)
theta2 = atand((2*(cotd(beta2))*((M2^2)*(sind(beta2))^2-1))/((gamma +
1)*(M2^2)-2*((M2^2)*(sind(beta2))^2-1)));
theta3 = atand((2*(cotd(beta3))*((M3^2)*(sind(beta3))^2-1))/((gamma +
1)*(M3^2)-2*((M3^2)*(sind(beta3))^2-1)));

% Theoretical Mach Numbers after each Oblique Shock.
M2_t = M1_n2/(sind(beta1-theta1));
M3_t = M2_n2/(sind(beta2-theta2));
M4_t = M3_n2/(sind(beta3-theta3));
```

```
 % Solving 5 Equations for 5 Unknowns. (Initial Guess: 2, 1.5, 30, 35, 45)
 solution = struct2cell(vpasolve([M1_n == M2_n, M1_n == M3_n, M4 == M4_t, M2 ==
M2_t, M3 == M3_t], [M2, M3, beta1, beta2, beta3], [2, 1.5, 30, 35, 45]));
 Ans = vertcat(subs(solution));
 %% Part 1 - Final Answers.
 clc
 % Calculated Mach Numbers Upstream of every Shock.
 M_1 = M1
 M_2 = double(Ans(1))
 M_3 = double(Ans(2))
 M_4 = M4
 M_5 = sqrt(((M4^2)+(2/(gamma-1)))/((((2*gamma)/(gamma-1))*(M4^2))-1))

 % Calculated Oblique Shock Wave Angles.
 beta_1 = double(Ans(3))
 beta_2 = double(Ans(4))
 beta_3 = double(Ans(5))
 beta_4 = 90

 % Calculated Oblique Shock Wave Deflection Angles.
 theta_1 = atand((2*(cotd(beta_1))*((M1^2)*(sind(beta_1))^2-1))/((gamma +
1)*(M1^2)-2*((M1^2)*(sind(beta_1))^2-1)))
 theta_2 = atand((2*(cotd(beta_2))*((M_2^2)*(sind(beta_2))^2-1))/((gamma +
1)*(M_2^2)-2*((M_2^2)*(sind(beta_2))^2-1)))
 theta_3 = atand((2*(cotd(beta_3))*((M_3^2)*(sind(beta_3))^2-1))/((gamma +
1)*(M_3^2)-2*((M_3^2)*(sind(beta_3))^2-1)))

 % Calculated Upstream Normal Components of Oblique Shocks.
 M_1n = M_1*sind(beta_1);
 M_2n = M_2*sind(beta_2);
 M_3n = M_3*sind(beta_3);
 M_4n = M4;

 % Calculated Static Pressure Ratios across all Shocks.
 P2_P1 = ((2*gamma*(M_1n)^2)/(gamma + 1)) - ((gamma - 1)/(gamma + 1))
 P3_P2 = (2*gamma*(M_2n)^2)/(gamma + 1) - (gamma - 1)/(gamma + 1)
 P4_P3 = (2*gamma*(M_3n)^2)/(gamma + 1) - (gamma - 1)/(gamma + 1)
 P5_P4 = (2*gamma*(M_4n)^2)/(gamma + 1) - (gamma - 1)/(gamma + 1)

 % Calculated Static Temperature Ratios across all Shocks.
 T2_T1 = ((1 + ((gamma - 1)/2)*(M_1n^2))*((((2*gamma)/(gamma - 1))*(M_1n^2))-
1))/((((gamma + 1)^2)/(2*(gamma - 1)))*(M_1n^2))
 T3_T2 = ((1 + ((gamma - 1)/2)*(M_2n^2))*((((2*gamma)/(gamma - 1))*(M_2n^2))-
1))/((((gamma + 1)^2)/(2*(gamma - 1)))*(M_2n^2))
 T4_T3 = ((1 + ((gamma - 1)/2)*(M_3n^2))*((((2*gamma)/(gamma - 1))*(M_3n^2))-
1))/((((gamma + 1)^2)/(2*(gamma - 1)))*(M_3n^2))
```

```
 T5_T4 = ((1 + ((gamma - 1)/2)*(M_4n^2))*((((2*gamma)/(gamma - 1))*(M_4n^2))-
1))/((((gamma + 1)^2)/(2*(gamma - 1)))*(M_4n^2))

 % Calculated Total Pressure Ratios across all Shocks.
 Po2_Po1 = (((0.5*(gamma + 1)*(M_1n)^2)/(1 + ((gamma -
1)/2)*(M_1n^2)))^(gamma/(gamma - 1)))*((1/(P2_P1))^(1/(gamma - 1)))
 Po3_Po2 = (((0.5*(gamma + 1)*(M_2n)^2)/(1 + ((gamma -
1)/2)*(M_2n^2)))^(gamma/(gamma - 1)))*((1/(P3_P2))^(1/(gamma - 1)))
 Po4_Po3 = (((0.5*(gamma + 1)*(M_3n)^2)/(1 + ((gamma -
1)/2)*(M_3n^2)))^(gamma/(gamma - 1)))*((1/(P4_P3))^(1/(gamma - 1)))
 Po5_Po4 = (((0.5*(gamma + 1)*(M_4n)^2)/(1 + ((gamma -
1)/2)*(M_4n^2)))^(gamma/(gamma - 1)))*((1/(P5_P4))^(1/(gamma - 1)))

 % Calculated Intake Pressure Recovery Ratio.
 Po5_Po1 = (Po2_Po1)*(Po3_Po2)*(Po4_Po3)*(Po5_Po4)
```

```
 %% Part 2 - Parametric Analysis.
 % clear
 % close
 % clc
```

Stations A to 1.

- Isentropic Flow
- Adiabatic
- $P_{oA} = P_{o1}$
- Cruise Altitude at 51,000 ft (Reference Below)
- [Maximum Cruise Altitude for Supersonic Turbojet Aircrafts.]

```
 % Station A - Ambient Conditions.
 u = symunit;                              % Declaring the Unit Variable.
 sympref('FloatingPointOutput',true);      % Displaying in Decimal Style.

 Altitude = 51000;                         % In Feet (15,544.8 Meters)
 P_amb = 11053.0*u.Pa                      % Ambient Pressure in Pa.
 T_amb = 216.650*u.K                       % Ambient Temperature in Kelvin.
 rho_amb = 0.177730*u.kg/u.m^3             % Ambient Density in Kg/m^3.
 a_amb = 295.070*u.m/u.s                   % In m/s (Speed of Sound).
 R = 287*u.J/(u.kg*u.K)                    % Gas Constant in J/Kg*K.
 gamma_d = 1.4;                            % Gamma for Diffuser.
 M_a = M_1;                                % Flight Mach No.

 % Station A - 1.
 V_amb = M_a*a_amb                         % Inlet Velocity.
```

```
 P_oA = unitConvert(((1 + ((gamma_d - 1)/(2))*M_a^2)^((gamma_d)/(gamma_d-
1)))*P_amb,u.kPa)
 P_o1 = P_oA ;                              % Isentropic Across Stations A - 1.
 T_oA = (1 + ((gamma_d - 1)/(2))*(M_a^2))*T_amb
 T_o1 = T_oA;                               % Adiabatic Across Stations A - 1.
```

Stations 1 to 2 --> Diffuser.

- Non - Isentropic Flow
- Non - Adiabatic
- Inlet Speeds are Supersonic, therefore a Series of Oblique shocks and then a Normal Skock Slow down the Flow
- $\pi_d = 0.9339 = \frac{P_{o2}}{P_{o1}}$ --> Calculated from Inlet Design Above
- Diffuser is Assumed to be at 100% Efficiency

```
 % Station 1 - 2 --> Diffuser.
 Pi_d = 0.9339;                                 % Diffuser Total Pressure Ratio
Calculated from Inlet Design.
 %eta_d = 0.9;                                  % Diffuser Efficiency.

 P_o2 = P_o1*Pi_d                               % Compressor Inlet Total
Pressure.
 theta_d = Pi_d^((gamma_d - 1)/(gamma_d));      % Diffuser Total Temperature
Ratio.
 T_o2 = T_o1*theta_d                            % Compressor Inlet Total
Temperature.

 P2_Pa = P5_P4*P4_P3*P3_P2*P2_P1;               % Static Pressure Ratio in
Diffuser.
 P_2 = unitConvert(P2_Pa*P_amb,u.kPa)           % Static Pressure at Compressor
Inlet.
 T2_Ta = T5_T4*T4_T3*T3_T2*T2_T1;               % Static Temperature Ratio in
Diffuser.
 T_2 = T2_Ta*T_amb                              % Static Temperature at
Compressor Inlet.
```

Stations 2 to 3 --> Compressor.

- Non - Isentropic Flow
- Non - Adiabatic
- $\pi_c = 11.89 = \frac{P_{o3}}{P_{o2}}$ (Reference Below)
- Assuming single compressor (HPC and LPC Combined)
- Concorde Engine for Compressor Ratio.
- $\eta_c = 0.9$ --> Compressor Effficiency

```
 % Station 2 - 3 --> Compressor.
 gamma_c = 1.37;                                                    % Gamma for
Compressor.
 Pi_c = 10;                                                         % Compressor
Total Pressure Ratio from Historic Data.
 eta_c = 0.9;                                                       % Compressor
Efficiency from Historic Data.

 Cp_c = unitConvert((gamma_c*R)/(gamma_c - 1),u.kJ/(u.kg*u.K))   % Specific Heat
Capacity for Compressor.
 P_o3 = unitConvert(P_o2*Pi_c,u.MPa)                                % Combustor
Inlet Total Pressure.
 theta_c = Pi_c^((gamma_c - 1)/(gamma_c));                          % Compressor
Total Temperature Ratio.
 T_o3 = T_o2*(1+(theta_c-1)/(eta_c))                                % Combustor
Inlet Total Temperature.
```

Stations 3 - 4 --> Combustion Chamber.

- Non - Isentropic Flow
- Non - Adiabatic
- $\pi_b = 0.95 = \frac{P_{o4}}{P_{o3}}$
- $Q_R = 43,390 \frac{\text{KJ}}{\text{Kg}}$ (Reference Below)
- Jet A Fuel Heating Value.
- $\eta_b = 0.95$ --> Combustion Chamber Efficiency
- $T_{o4} = 1800\,K.$
- Combustion Chamber Exit Temperature (Based on Turbine Blade Material Limit)

```
 % Station 3 - 4 --> Combustor Chamber.
 gamma_b = 1.35;                                    % Gamma for Combustor.
 Pi_b = 0.95;                                       % Combustor Total Pressure
Ratio.
 eta_b = 0.99;                                      % Combustor Efficieny.
 Q_r = 43390*u.kJ/u.kg                              % Jet A Fuel Heating Value.
 T_o4 = 1300*u.K                                    % Turbine Inlet Total
Temperature - Turbine Blade Temperature Limit.

 P_o4 = P_o3*Pi_b                                   % Turbine Inlet Total Pressure.
 Cp_b_avg = (gamma_b*R)/(gamma_b - 1)               % Average Specific Heat
Capacity for Combustor.
 Cp_b_e = unitConvert(2*Cp_b_avg,u.kJ/(u.kg*u.K))  - Cp_c                    %
Exit Specific Heat Capacity for Combustor.
```

```
 theta_b = Pi_b^((gamma_b - 1)/(gamma_b));       % Combustor Total Temperature
Ratio.
 f_b = ((T_o4/T_o3)-(Cp_c/Cp_b_e))/(((Q_r*eta_b)/(Cp_b_e*T_o3))-(T_o4/T_o3))
```

Station 4 - 5 --> Turbine.

- Non - Isentropic Flow
- Non - Adiabatic
- $\eta_t = 0.95$ --> Turbine Efficiency.

```
 % Station 4 - 5 --> Turbine.
 gamma_t = 1.33;                                                          %
Gamma for Turbine.
 eta_t = 0.95;                                                            %
Turbine Efficiency.
 eta_m = 0.99;

 T_o5 = T_o4 - (T_o3 - T_o2)/(eta_m)                                      %
Turbine Exit Total Temperature.
 P_o5 = unitConvert(P_o4*((1 - ((T_o4 - T_o5)/(eta_t*T_o4)))^((gamma_t)/(gamma_t
- 1))),u.kPa)  % Turbine Exit Total Pressure.
```

Station 5 - 6 --> Afterburner.

- Non - Isentropic Flow
- Non - Adiabatic
- $\eta_{ab} = 0.95$ --> Afterburner Efficiency.
- $\pi_{ab} = 0.95 = \frac{P_{o6}}{P_{o5}}$
- $T_{o6} = 2500\,K$.

```
 % Station 5 - 6 --> Afterburner.
 gamma_ab = 1.33;
% Gamma for Afterburner.
 Pi_ab = 0.95;
% Afterburner Total Pressure Ratio.
 eta_ab = 0.95;
% Afterburner Efficiency.
 T_o6 = 1500*u.K
% Temperature Limit at Afterburner Exit.

 P_o6 = Pi_ab*P_o5
% Afterburner Exit Total Pressure.
 Cp_t = (gamma_ab*R)/(gamma_ab - 1);
% Specific Heat Capacity for Turbine.
```

```
 Cp_ab = Cp_t;
% Specific Heat Capacity for Afterburner.
 f_ab = ((T_o6/T_o5)-
(Cp_t/Cp_ab))/(((unitConvert(Q_r,u.J/(u.K*u.kg))*eta_ab)/(Cp_ab*T_o5))-
(T_o6/T_o5))
```

Station 6 - e --> Nozzle.

- Fully expanded Nozzle
- Isentropic Flow

```
 % Station 5 - 7 --> Nozzle.
 eta_n = 0.98;                                          % Nozzle Efficieny.
 gamma_n = 1.36;                                        % Gamma for Nozzle.
 A_inlet = 2.2*u.m^2                                    % Assumed Inlet
Area in m^2.
 A_exit = 0.75*u.m^2                                    % Assumed Inlet
Area in m^2.
 M_e = 2.621

 P_e = P_o6/(((1 + ((gamma_n - 1)/(2))*M_e^2)^((gamma_n)/(gamma_n-1))))
 A_throat = A_exit/((1/M_e)*((2/(gamma_n + 1))*(1 + ((gamma_n -
1)/2)*(M_e^2))^((gamma_n + 1)/(2*(gamma_n - 1)))))
 T_e = T_o6/(1 + ((gamma_n - 1)/2)*(M_e^2))
 V_e = M_e*sqrt(gamma_n*unitConvert(R,u.m^2/(u.K*u.s^2))*T_e)

 Ae_mdot = simplify((((gamma_n + 1)/2)^(1/(gamma_n - 1)))*(((gamma_n +
1)/(2*gamma_n*unitConvert(R,u.m^2/(u.K*u.s^2))*T_o6))^(0.5))*((unitConvert(R,u.m
^2/(u.K*u.s^2))*T_o6)/unitConvert(P_o6,u.kg/(u.m*u.s^2))))
```

Performance Calculations

- Specific Thrust
- TSFC
- $\dot{M}_a$
- Thrust
- η_{th} = 30-50%
- η_p = 70-80%
- η_{Overall}

```
 % Performance Criteria.
 %f_ab = 0;
 Specific_Thrust = (1 + f_b + (1 + f_b)*f_ab)*V_e - V_amb +
Ae_mdot*(unitConvert(P_e,u.kg/(u.m*u.s^2)) -
unitConvert(P_amb,u.kg/(u.m*u.s^2)))*(1 + f_b + (1 + f_b)*f_ab)
```

```
 TSFC = (f_b + (1 + f_b)*f_ab)/Specific_Thrust

 mdot_a = rho_amb*A_inlet*V_amb          % Mass Flow Rate of Air at Inlet.
 mdot_f = mdot_a*(f_b + (1 + f_b)*f_ab)  % Total Mass Flow Rate of Fuel(burner +
afterburner).
 mdot_e = mdot_a + mdot_f                % Mass Flow Rate of Air at Exit.
 rho_e =
unitConvert(P_e,u.kg/(u.m*u.s^2))/(unitConvert(R,u.m^2/(u.K*u.s^2))*T_e) %
Nozzle Exit Density.
 Thrust_net = separateUnits(Specific_Thrust*mdot_a/1000)*u.kN   % Thrust.
 Thrust_gross = unitConvert((1 + f_b + (1 + f_b)*f_ab)*V_e*mdot_a,u.kN)

 eta_th = 100*(((1 + f_b + (1 + f_b)*f_ab)*((V_e^2)/2) - (V_amb^2/2))/((f_b + (1
+ f_b)*f_ab)*unitConvert(Q_r,u.m^2/u.s^2)))
 eta_p = 100*((Specific_Thrust*V_amb)/((1 + f_b + (1 + f_b)*f_ab)*((V_e^2)/2) -
(V_amb^2/2)))
 eta_overall = eta_th*eta_p/100          % Overall Efficiency.
 % Inlet Geometry Rendition.
 % Angle and Length Calculations.

 Inlet_Radius = sqrt(separateUnits(A_inlet)/pi)
 Exit_Radius = sqrt(A_exit)/pi
 Throat_Radius = sqrt(A_throat)/pi

 % Length of the Shock Wave.
 Lm1 = Inlet_Radius * sind(90)/sind(beta_1);
 Lm2 = Lm1 * sind(beta_1 - theta_1)/sind(180 - beta_2);
 Lm3 = Lm2 * sind(beta_2 - theta_2)/sind(180 - beta_3);
 Lm4 = Lm3 * sind(beta_3 - theta_3)/sind(beta_4);

 % Length of the deflection line.
 wm1 = Lm1 * sind(beta_2 - beta_1 + theta_1)/sind(180 - beta_2);
 wm2 = Lm3 * sind(beta_3 - beta_2 + theta_2)/sind(beta_2 - theta_2);
 wm3 = Lm4 * sind(beta_4 - beta_3 + theta_3)/sind(beta_3 - theta_3);

 % Creating lines
 x = 0;
 y = 0;

 % Oblique Shock 1
 L1 = Lm1;
 alpha1 = beta_1;
 x1 = x + (L1 * cosd(alpha1));
 y1 = y + (L1 * sind(alpha1));

 % Deflection line 1
```

```
L3 = wm1;
alpha3 = theta_1;
x3 = x + (L3 * cosd(alpha3));
y3 = y + (L3 * sind(alpha3));

% Oblique Shock 2
L4 = Lm2;
alpha4 = beta_2 + theta_1;
x4 = x3 + (L4 * cosd(alpha4));
y4 = y3 + (L4 * sind(alpha4));

% Deflection line 2
L5 = wm2;
alpha5 = theta_2 + theta_1;
x5 = x3 + (L5 * cosd(alpha5));
y5 = y3 + (L5 * sind(alpha5));

% Oblique Shock 3
L6 = Lm3;
alpha6 = beta_3 + theta_1 + theta_2;
x6 = x5 + (L6 * cosd(alpha6));
y6 = y5 + (L6 * sind(alpha6));

% Deflection line 3
L7 = wm3;
alpha7 = theta_3 + theta_1 + theta_2;
x7 = x5 + (L7 * cosd(alpha7));
y7 = y5 + (L7 * sind(alpha7));

% Normal Shock
L8 = Lm4;
alpha8 = theta_3 + theta_1 + theta_2 + beta_4;
x8 = x7 + (L8 * cosd(alpha8));
y8 = y7 + (L8 * sind(alpha8));
close
% Plotting the points to shape the inlet wedge.
%ylim([-0.8 0.8])
%xlim([0 3.1])
figure (1)
h = gca;
h.XAxis.Visible = 'off';
h.YAxis.Visible = 'off';
hold on

% Top Side
plot([x x1],[y y1])        % Oblique shock 1
```

```
 plot([x x3],[y y3])          % deflection line

 plot([x3 x4],[y3 y4])       % Oblique shock 2
 plot([x3 x5],[y3 y5])        % deflection line

 plot([x5 x6],[y5 y6])       % Oblique shock 3
 plot([x5 x7],[y5 y7])        % deflection line

 plot([x7 x8],[y7 y8])       % Normal Shock

 % Bottom Side
 plot([x x1],[-y -y1])       % Oblique shock 1
 plot([x x3],[-y -y3])        % deflection line

 plot([x3 x4],[-y3 -y4])     % Oblique shock 2
 plot([x3 x5],[-y3 -y5])      % deflection line

 plot([x5 x6],[-y5 -y6])     % Oblique shock 3
 plot([x5 x7],[-y5 -y7])      % deflection line

 plot([x7 x8],[-y7 -y8])     % Normal Shock
```

```
 % Station Lines

 plot([0 0],[-1 1],"-.")      % Ambient --> a.
 text(0.1,-0.9,'a','HorizontalAlignment','center')

 plot([x1 x1],[-1 1],"-.")    % Inlet --> 1.
 text(1.45,-0.9,'1','HorizontalAlignment','center')
 td = text(1.75,0,'Inlet &
Diffuser','HorizontalAlignment','center','FontWeight','Bold');
 td.Rotation = 90;

 plot([2.3 2.3],[-1 1],"-.") % Compressor Inlet --> 2.
 text(2.5,-0.9,'2','HorizontalAlignment','center')
 ct =
text(3.15,0,'Compressor','HorizontalAlignment','center','FontWeight','Bold');
 ct.Rotation = 90;

 plot([4 4],[-1 1],"-.")      % Combustor Inlet --> 3.
 text(4.2,-0.9,'3','HorizontalAlignment','center')
 bt = text(4.5,0,'Burner','HorizontalAlignment','center','FontWeight','Bold');
 bt.Rotation = 90;
```

```
plot([5 5],[-1 1],"-.")     % Turbine Inlet --> 4.
text(5.2,-0.9,'4','HorizontalAlignment','center')
tt = text(5.25,0,'Turbine','HorizontalAlignment','center','FontWeight','Bold');
tt.Rotation = 90;

plot([5.5 5.5],[-1 1],"-.") % Afterburner Inlet --> 5.
text(5.7,-0.9,'5','HorizontalAlignment','center')
abt = text(6,0,'A/B','HorizontalAlignment','center','FontWeight','Bold');
abt.Rotation = 90;

plot([6.5 6.5],[-1 1],"-.")     % Nozzle Inlet --> 6.
text(6.7,-0.9,'6','HorizontalAlignment','center')
nt = text(8.25,0,'Nozzle','HorizontalAlignment','center','FontWeight','Bold');
nt.Rotation = 90;

plot([10 10],[-1 1],"-.")     % Nozzle Exit --> e.
text(10.2,-0.9,'e','HorizontalAlignment','center')

plot([x8 6.5],[y8 y8])            % Top Horizontal Line
plot([x8 6.5],[-y8 -y8])          % Bottom Horizontal Line
plot([x7 x7],[y7 -y7])         % Wedge Vertical Line

plot([6.5 9],[Inlet_Radius 0.1296])     % Converging Top Line
plot([6.5 9],[-Inlet_Radius -0.1296])   % Converging Bottom Line

plot([9 10],[0.1296 0.2757])     % Diverging Top Line
plot([9 10],[-0.1296 -0.2757])   % Diverging Bottom Line

plot([10 10],[0.2757 -0.2757])   % Vertical Line at Exit

%xlabel('Engine Section')
title('Supersonic Turbojet Engine with an Afterburner.')
hold off
```

```
% Plotting Pressure Across the Engine.
close
clc
figure (2)


j = gca;
j.XAxis.Visible = 'off';
yyaxis Left
```

```
 plot([0 0],[100 1600],"-.");     % Ambient --> a.
 hold on
 text(0,50,'a','HorizontalAlignment','center');
 td = text(1.75,800,'Inlet &
Diffuser','HorizontalAlignment','center','FontWeight','Bold');
 td.Rotation = 90;
 plot ([0 x1],[separateUnits(P_oA) separateUnits(P_o1)],"-");

 plot([x1 x1],[100 1600],"-.")   % Inlet --> 1.
 text(x1,50,'1','HorizontalAlignment','center')
 ct =
text(3.15,800,'Compressor','HorizontalAlignment','center','FontWeight','Bold');
 ct.Rotation = 90;
 plot ([x1 2.3],[separateUnits(P_o1) separateUnits(P_o2)],"-");

 plot([2.3 2.3],[100 1600],"-.") % Compressor Inlet --> 2.
 text(2.3,50,'2','HorizontalAlignment','center')
 bt = text(4.5,800,'Burner','HorizontalAlignment','center','FontWeight','Bold');
 bt.Rotation = 90;
 plot ([2.3 4],[separateUnits(P_o2) separateUnits(P_o3*1000)],"-");

 plot([4 4],[100 1600],"-.")     % Combustor Inlet --> 3.
 text(4,50,'3','HorizontalAlignment','center')
 tt =
text(5.25,800,'Turbine','HorizontalAlignment','center','FontWeight','Bold');
 tt.Rotation = 90;
 plot ([4 5],[separateUnits(P_o3*1000) separateUnits(P_o4*1000)],"-");

 plot([5 5],[100 1600],"-.")     % Turbine Inlet --> 4.
 text(5,50,'4','HorizontalAlignment','center')
 abt = text(6,800,'A/B','HorizontalAlignment','center','FontWeight','Bold');
 abt.Rotation = 90;
 plot ([5 5.5],[separateUnits(P_o4*1000) separateUnits(P_o5)],"-");

 plot([5.5 5.5],[100 1600],"-.") % Afterburner Inlet --> 5.
 text(5.5,50,'5','HorizontalAlignment','center')
 nt =
text(8.25,800,'Nozzle','HorizontalAlignment','center','FontWeight','Bold');
 nt.Rotation = 90;
 plot ([5.5 6.5],[separateUnits(P_o5) separateUnits(P_o6)],"-");


 plot([6.5 6.5],[100 1600],"-.")     % Nozzle Inlet --> 6.
 text(6.5,50,'6','HorizontalAlignment','center')
 plot ([6.5 10],[separateUnits(P_o6) separateUnits(P_o6)],"-");
```

```
plot([10 10],[100 1600],"-.")     % Nozzle Exit --> e.
text(10,50,'e','HorizontalAlignment','center')

ylim([100 1600])
ylabel('Stagnation Pressure [kPa]')

yyaxis Right
ylabel('Stagnation Temperature [K]')
plot ([0 x1],[separateUnits(T_oA) separateUnits(T_o1)],"-");
plot ([x1 2.3],[separateUnits(T_o1) separateUnits(T_o2)],"-");
plot ([2.3 4],[separateUnits(T_o2) separateUnits(T_o3)],"-");
plot ([4 5],[separateUnits(T_o3) separateUnits(T_o4)],"-");
plot ([5 5.5],[separateUnits(T_o4) separateUnits(T_o5)],"-");
plot ([5.5 6.5],[separateUnits(T_o5) separateUnits(T_o6)],"-");
plot ([6.5 10],[separateUnits(T_o6) separateUnits(T_o6)],"-");
ylim([400 1600])

%xlabel('Engine Section')
title('Stagnation Condition across the Engine.')

hold off
```